ELSEVIER

# Low-frequency damping properties of near-stoichiometric Ni₂MnGa shape memory alloys under isothermal conditions

S.H. Chang[a] and S.K. Wu[b,*]

[a]Department of Chemical and Materials Engineering, National I-Lan University, I-Lan 260, Taiwan
[b]Department of Materials Science and Engineering, National Taiwan University, 1 Roosevelt Road Sec. 4, Taipei 106, Taiwan

The low-frequency damping properties of near-stoichiometric Ni₂MnGa shape memory alloys were investigated by dynamic mechanical analysis. Ni₂MnGa alloys can possess good inherent internal friction under isothermal conditions over a wide temperature range from $-100$ to $100\,^{\circ}\mathrm{C}$ without deterioration after thermal cycling. Ni₂MnGa alloys with higher martensitic transformation temperatures are candidates for high damping applications since they can possess good inherent internal friction above room temperature.
© 2008 Acta Materialia Inc. Published by Elsevier Ltd. All rights reserved.

*Keywords:* Ni–Mn–Ga shape memory alloys; Martensitic phase transformation; Internal friction; Dynamic mechanical analyzer

Shape memory alloys (SMAs) exhibiting a thermoelastic martensitic transformation can show unique properties including the shape memory effect (SME) and superelasticity [1]. Meanwhile, during the martensitic transformation or in the martensite state, SMAs usually possess good internal friction (IF) and are potential candidates for high damping applications [2–5]. When heating and cooling SMAs, there is an IF peak with a storage modulus ($E_0$) minimum appearing at the martensitic transformation temperature [3]. The IF peak of SMAs can be decomposed into three individual terms: $IF_{Tr}$, $IF_{PT}$ and $IF_{I}$ [6,7]. The first term, $IF_{Tr}$, is the transitory IF which appears only at low-frequency ($\upsilon$) and non-zero cooling/heating rate $\dot{T}$. The second term, $IF_{PT}$, is the inherent IF corresponding to phase transformation, and is independent of $\dot{T}$. The third term, $IF_{I}$, is the intrinsic IF of the austenitic or martensitic phase and depends strongly on microstructural properties such as dislocations, vacancies and twin boundaries. In the low-frequency range, the IF peak observed during transformation is mainly ascribed to the first term, $IF_{Tr}$. However, the damping capacity of $IF_{Tr}$ usually decreases instantly when $\dot{T}$ is abruptly stopped and only $IF_{PT} + IF_{I}$ persists [8]. Therefore, it is more important to consider the damping property of $IF_{PT} + IF_{I}$ since, for most engineering applications, these high-damping SMAs are used at a set temperature (generally around room temperature), instead of a constant $\dot{T}$. The damping characteristics of $IF_{PT} + IF_{I}$ during martensitic transformation of $Ti_{50}Ni_{50}$ and $Ti_{51}Ni_{39}Cu_{10}$ SMAs have been systematically studied by dynamic mechanical analysis (DMA) [8,9]. Both these TiNi-based SMAs exhibit good $IF_{PT} + IF_{I}$ ($\tan \delta > 0.02$) during martensitic transformation under isothermal conditions. Near-stoichiometric Ni₂MnGa SMAs also undergo a martensitic transformation during cooling/heating and show a ferromagnetic transition near $100\,^{\circ}\mathrm{C}$ [10,11]. Chernenko et al. [12] indicated that the martensitic transformation temperature ($M_s$) of Ni–Mn–Ga SMAs is highly sensitive to their chemical composition. Wu and Yang [13] showed that Ni–Mn–Ga SMAs can exhibit a wide range of $M_s$ temperature from $-120$ to $185\,^{\circ}\mathrm{C}$ by controlling their chemical composition. Therefore, it can be expected that Ni–Mn–Ga SMAs could possess high inherent IF at room temperature if their $M_s$ temperatures are adjusted to near room temperature. In this study, three different types of near-stoichiometric Ni₂MnGa SMAs are investigated by DMA to examine their inherent IF under isothermal conditions. The damping characteristics of these Ni–Mn–Ga SMAs are also discussed and compared to those of the $Ti_{50}Ni_{50}$ and $Ti_{51}Ni_{39}Cu_{10}$ SMAs examined in our previous studies.

---

* Corresponding author. Tel.: +886 2 2363 7846; fax: +886 2 2363 4562; e-mail: skw@ntu.edu.tw

**Table 1.** Chemical compositions (at.%), phase transformation ($T_I$ & $T_M$) and Curie ($T_C$) temperatures (°C) for Groups I - III Ni-Mn-Ga SMAs. $T_I$ and $T_M$ are the transformation temperatures corresponding to parent to intermediate (P→I) and intermediate to martensite or parent to martensite (I→M or P→M), respectively

| Alloy | at.% Ni | at.% Mn | at.% Ga | $T_I$ (°C) | $T_M$ (°C) | $T_C$ (°C) |
|---|---|---|---|---|---|---|
| Group I | 50.66 | 26.89 | 22.30 | −22.5 | −55.9 | 93.7 |
| Group II | 52.04 | 26.51 | 21.35 | — | 6.9 | 79.3 |
| Group III | 53.72 | 26.80 | 19.32 | — | 129.8 | 64.0 |

Near-stoichiometric $Ni_2MnGa$ SMAs ingots used in this study were prepared by vacuum arc remelting from the raw materials of Ni (purity 99.9 wt.%), Mn55–Ni45 mother alloy (in wt.%) and Ga (purity 99.9 wt.%), followed by homogenizing at 850 °C for 48 h. The homogenized ingots were then cut using a low-speed diamond saw for electron probe microanalysis (EPMA) and DMA tests. The compositions of homogenized near-stoichiometric $Ni_2MnGa$ SMAs were determined by EPMA using a JEOL JXA-8600SX microscope [13]. Specimens for the DMA experiment were also cut from the homogenized ingots to dimensions of $20.0 \times 3.3 \times 2.8$ mm$^3$. Tan $\delta$ and $E_0$ values for each specimen were measured by TA 2980 DMA equipment using $\dot{T} = 3$ °C min$^{-1}$, $\upsilon = 1$ Hz and amplitude $\sigma_0 = 5$ μm (strain amplitude $= 1.1 \times 10^{-4}$). All DMA measurements in this study were conducted without applying a magnetic field. Table 1 lists the chemical compositions measured by EPMA for the three near-stoichiometric $Ni_2MnGa$ SMAs specimens used in this study. The inherent IF ($IF_{PT} + IF_I$) of each specimen was also measured using TA 2980 DMA equipment under isothermal conditions. The detailed procedure for the isothermal DMA test was described in Ref. [8].

Figure 1a and b show the DMA $E_0$ and tan $\delta$ curves, respectively, as a function of temperature for solution-treated Ni–Mn–Ga SMAs. Only the cooling curves are shown in detail. As illustrated in Figure 1a, the Curie point, $T_c$, for each specimen can be determined by the change in slope of the $E_0$ curve because there is a discontinuous behavior of $E_0$ curve caused by the indirect interaction between magnetization and soft phonon potential at this temperature [14]. Meanwhile, as shown in Figure 1b, transformation temperatures of each specimen can be obtained from the IF peak temperature of the tan $\delta$ curve. All the characteristic temperatures noted in Figure 1, such as the Curie point temperature $T_c$, temperatures for parent to intermediate phase (P → I, $T_I$), intermediate to martensite or parent to martensite (I → M or P → M, $T_M$), are listed in Table 1. According
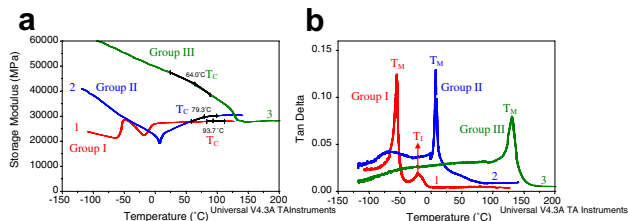
to the classification of Ni–Mn–Ga SMAs reported by Chernenko et al. [12,14], curve 1 can be classified as Group I Ni–Mn–Ga SMA because its $T_M$ temperature is well below room temperature and $T_C$. In addition, curve 2 can be categorized as Group II SMA since its $T_M$ temperature is close to room temperature but below $T_C$. Curve 3 can be labeled as Group III SMA due to its high $T_M$ temperature (above $T_C$). As shown in Figure 1b, the IF peaks for Groups I and II SMAs exhibit a high tan $\delta$ value above 0.11, while that for Group III SMA shows only a value lower than about 0.08. This feature arises from the fact that, during martensitic transformation, Group III SMA exhibits a higher $E_0$ minimum (27,600 MPa) than Group I SMA (21300 MPa) and Group II SMA (19,100 MPa) and does not show a conspicuous softening. In addition, in Figure 1b, the IF peak of Group I SMA at $T_I$ temperature only has a low tan $\delta$ value (about 0.02) during cooling. This is due to the fact that the parent to intermediate phase transformation (P → I) is only associated with a soft $1/3TA_2$ phonon mode condensation, instead of a significant martensitic transformation (P → M or I → M) with structural change [14,15]. Except for the aforementioned transformation peaks, an extra broad peak can also be observed in the tan $\delta$ curve of Group II SMA at about −75 °C. This extra peak does not accompany a significant $E_0$ drop and is known as the relaxation peak [3]. The relaxation peak is also observed in IF results of Ni–Mn–Ga SMAs reported by Seguí et al. [16]. Recently, Fan et al. [17] revealed that the relaxation peak of TiNi SMAs originates from the interaction between twin boundaries and hydrogen and is also affected by dislocations. The damping mechanism of the relaxation peak appearing in Ni–Mn–Ga SMAs may be similar to that of TiNi SMAs, though further study is needed to elucidate its characteristics.

Figure 2 plots the tan $\delta$ values vs. isothermal interval (0–30 min) of Groups I–III Ni–Mn–Ga SMAs kept isothermally at each transformation peak temperature ($T_I$
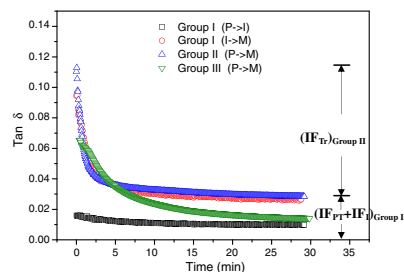


**Figure 1.** (a) Storage modulus $E_0$ and (b) tan $\delta$ curves measured at $\dot{T} = 3$ °C min$^{-1}$, $\upsilon = 1$ Hz and $\sigma_0 = 5$ μm for Groups I–III Ni–Mn–Ga SMAs.



**Figure 2.** Tan $\delta$ values vs. isothermal time interval for Figure 1 specimens measured at $\upsilon = 1$ Hz, $\sigma_0 = 5$ μm under isothermal conditions around the transformation temperature.

or $T_M$). As shown in Figure 2, tan $\delta$ values of these Ni–Mn–Ga SMAs all decrease with prolonged isothermal time and reach a steady value after 30 min. As illustrated in Figure 2, the decayed tan $\delta$ value during isothermal treatment represents the $IF_{Tr}$ which is associated with the magnitude of $\dot{T}$. The steady tan $\delta$ value after isothermal treatment is the $IF_{PT} + IF_I$ during phase transformation, which is independent of $\dot{T}$. Note that tan $\delta$ values of $IF_{Tr}$ for Groups I and II SMAs collapse much faster than that of Group III, i.e. 95% of $IF_{Tr}$ for Groups I and II SMAs diminishes within 12 min but this takes 20 min for Group III SMAs. In addition, as shown in Figure 2, the $IF_{Tr}$ for the P → I peak at $T_I$ in Group I SMAs is insignificant compared to the $IF_{Tr}$ of the P → M or I → M transformations. This phenomenon agrees with the fact that P → I transformation does not correspond to the thermally induced martensitic transformation which mainly contributes to the $IF_{Tr}$ peak in the tan $\delta$ curve.

In order to investigate the inherent IF, $IF_{PT} + IF_I$, of Ni–Mn–Ga SMAs, DMA tan $\delta$ tests under 30 min isothermal treatment at different temperatures for Groups I–III SMAs were conducted, and the results are indicated in Figure 3a–c, respectively. As shown in Figure 3, the solid lines represent the tan $\delta$ cooling curve measured at $\dot{T} = 3\,°C\,min^{-1}$ (same as those shown in Fig. 1b) and the empty circles symbolize tan $\delta$ values of inherent IF measured by isothermal DMA tests. In Figure 3a, Group I SMAs show a higher $(IF_{PT} + IF_I)_{I \to M}$ peak with a tan $\delta$ value of 0.027 at $T_M$, and have a lower $(IF_{PT} + IF_I)_{P \to I}$ peak with a tan $\delta$ value of 0.011 at $T_I$. In Figure 3b and c, Groups II and III SMAs show a $(IF_{PT} + IF_I)_{P \to M}$ peak with tan $\delta$ values of 0.029 and 0.016, respectively. As shown in Figure 3, there is a small temperature deviation between the $IF_{PT} + IF_I$ peak and the IF peak for each specimen. This temperature shift is due to the cooling rate effect, which has been described in detail elsewhere [18]. When each specimen is isothermally treated (i.e. $\dot{T} = 0$) at around the transfor-

mation temperature, the tan $\delta$ value of $IF_{Tr}$ disappears gradually and only $IF_{PT} + IF_I$ term persists. This behavior is similar to that observed in $Ti_{50}Ni_{50}$ SMA [8]. Therefore, the damping capacity of $IF_{PT} + IF_I$ for Ni–Mn–Ga SMAs is proposed to be originated from stress-assisted martensitic transformation and stress-assisted motions of twin boundaries generated during martensitic transformation. Meanwhile, as illustrated in Figure 3, Group II SMAs show the highest $IF_{PT} + IF_I$ peak (tan $\delta = 0.030$) compared with Group I (tan $\delta = 0.026$) and Group III (tan $\delta = 0.016$) SMAs. Recently, Böhm et al. [19] revealed that $Ni_{50}Mn_{30}Ga_{20}$ SMA can exhibit either 5 M or 7 M martensite after plastic deformation and heat treatment. In addition, it has been reported that the twin boundaries of 5 M martensite possess higher mobility and can dissipate more energy during damping [14,20]. Therefore, from Figure 3, we suggested that 5 M martensite is more dominant in Group II Ni–Mn–Ga SMAs after martensitic transformation. However, more detailed investigation on the relation between martensite structure and its damping capacity is needed. Furthermore, from Figure 3, we can calculate the individual contribution of $IF_{Tr}$ and $IF_{PT} + IF_I$ to the overall IF peak. In this study, the contribution of $IF_{PT} + IF_I$ to overall IF for Group I, II and III SMAs is calculated as 23.5%, 23.5% and 20.5%, respectively. These values are comparable to those of $Ti_{50}Ni_{50}$ SMA (18.5% for B2 → R and 22.3% for R → B19′ martensitic transformations) [8] and solution-treated $Ti_{51}Ni_{39}Cu_{10}$ SMAs (17.2% for B2 → B19 and 20.0% for B19 → B19′ martensitic transformations) [9] under the same experimental parameters $(\dot{T}) = 3\,°C\,min^{-1}$, $\upsilon = 1$ Hz and $\sigma_0 = 5\,\mu m$). However, these values are lower than those of the off-stoichiometric $Ni_2MnGa$ SMAs reported by Seguí et al., i.e. 40% [16]. This deviation may be due to the insufficient isothermal time interval (only 15 min) and the improper step-cooling method (stoping every other 5 °C in cooling) used by Seguí et al. [16,21].

Figure 4a and b plot the inherent tan $\delta$ and $E_0$ curves, respectively, for Groups I–III Ni–Mn–Ga SMAs measured by isothermal DMA tests as well as those for $Ti_{50}Ni_{50}$ [8] and $Ti_{51}Ni_{39}Cu_{10}$ [9] SMAs. The experimental parameters used for each specimen in Figure 4 are all the same ($\upsilon = 1$ Hz and $\sigma_0 = 5\,\mu m$). As shown in Figure 4a, $Ti_{51}Ni_{39}Cu_{10}$ alloy has the highest $IF_{PT} + IF_I$ peak height (tan $\delta > 0.035$) during the B19 → B19′ martensitic transformation (at about 10 °C) at the first round
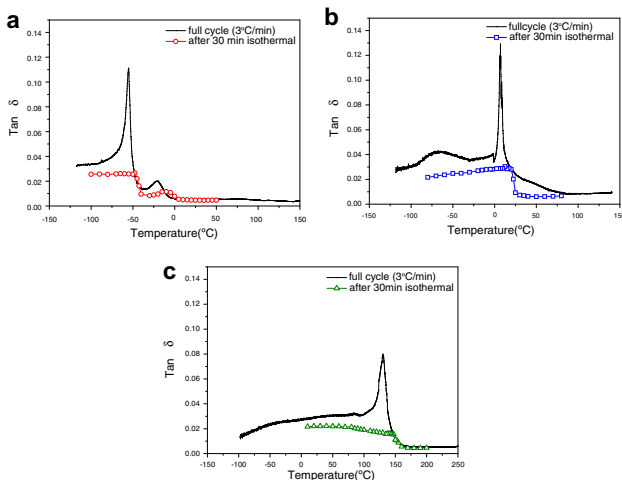


**Figure 3.** Tan $\delta$ values vs. temperature for (a) Group I, (b) Group II and (c) Group III SMAs measured at $\upsilon = 1$ Hz, $\sigma_0 = 5\,\mu m$. The solid curves are measured at $\dot{T} = 3\,°C\,min^{-1}$ and the empty symbol curves are the tan $\delta$ values of each specimen measured after 30 min isothermal treatment.
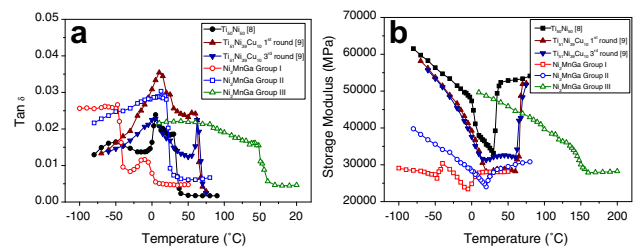


**Figure 4.** (a) Tan $\delta$ and (b) storage modulus $E_0$ values of Groups I–III Ni–Mn–Ga SMAs, cold-rolled $Ti_{50}Ni_{50}$ SMA annealed at 650 °C for 2 min [8], solution-treated $Ti_{51}Ni_{39}Cu_{10}$ SMA [9] measured after 30 min isotherm treatment at different temperatures.
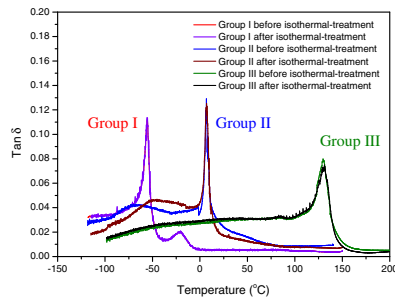
**Figure 5.** Tan $\delta$ curves for Groups I–III Ni–Mn–Ga SMAs measured before (from Fig. 1b) and after 30 min isothermal DMA tests.

of 30 min isothermal treatment, but this peak height decreases to 0.023 at the third round. The decreasing tan $\delta$ value of $IF_{PT} + IF_I$ is associated with the increasing defects or dislocations introduced by repeated thermal cycling during the isothermal treatment at different temperatures. The introduced defects or dislocations impede the stress-assisted transformation and the mobility of twin boundaries in martensite and hence lower the damping capacity [9]. In addition, $Ti_{50}Ni_{50}$ SMA also possesses good inherent IF (tan $\delta > 0.02$) but only over a very narrow temperature range during the $R \rightarrow B19'$ transformation (from 2 to 15 °C). The reason is that $R \rightarrow B19'$ transformation exhibits larger transformation strain and has more twin boundaries than the $B2 \rightarrow R$ one and thus can dissipate more damping energy.

Compared with $Ti_{50}Ni_{50}$ SMA, as shown in Figure 4a, Groups I–III Ni–Mn–Ga SMAs also process good inherent damping capacities (tan $\delta > 0.02$) since they all exhibit low inherent $E_0$ values during transformation, as shown in Figure 4b. Moreover, Groups I–III Ni–Mn–Ga SMAs can exhibit good inherent IF in a wider temperature range (from $-100$ to $100$ °C) than $Ti_{50}Ni_{50}$ SMA. This feature comes from the fact that Groups I–III Ni–Mn–Ga SMAs exhibit conspicuous damping capacities not only during martensitic transformation but also in the martensite state. Figure 5 plots the cooling tan $\delta$ curves for the same specimens of Groups I–III Ni–Mn–Ga SMAs measured before (from Fig. 1b) and after isothermal tests so as to investigate the thermal cycling effect on their damping capacities. As shown in Figure 5, tan $\delta$ curves for Groups I–III SMAs before and after isothermal treatments are very similar, apart from a deviation in the relaxation peak of Group II SMAs. This phenomenon reflects that, after a number of thermal cycles, the damping capacity for Ni–Mn–Ga SMAs deteriorates less seriously than for $Ti_{51}Ni_{39}Cu_{10}$ SMA. In conclusion, Groups II and III

Ni–Mn–Ga SMAs can exhibit and maintain a high damping capacity, comparable to that of $Ti_{50}Ni_{50}$ and $Ti_{51}Ni_{39}Cu_{10}$ SMAs, even after repeating thermal cycles. Nevertheless, the undesirable brittle characteristic of Ni–Mn–Ga SMAs critically limits their workability and need to be overcome before these can serve as high-damping materials.

[1] C.M. Wayman, T.W. Duerig, in: T.W. Duerig, K.N. Melton, D. Stöckel, C.M. Wayman (Eds.), Engineering Aspects of Shape Memory Alloys, Butterworth-Heinemann, London, 1990, pp. 3–20.
[2] O. Mercier, K.N. Melton, Y. De Préville, Acta Metall. 27 (1979) 1467.
[3] S.K. Wu, H.C. Lin, T.S. Chou, Acta Metall. 38 (1990) 95.
[4] K. Sugimoto, T. Mori, K. Otsuka, K. Shimizu, Scr. Metall. 8 (1974) 1341.
[5] B. Coluzzi, A. Biscarini, R. Campanella, L. Trotta, G. Mazzolai, A. Tuissi, F.M. Mazzolai, Acta Mater. 47 (1999) 1965.
[6] W. Dejonghe, R. De Batist, L. Delaey, Scr. Metall. 10 (1976) 1125.
[7] J. Van Humbeek, J. Stoiber, L. Delaey, R. Gotthardt, Z. Metalkd, Zeitschrift Fur Metallkunde 86 (1995) 176.
[8] S.H. Chang, S.K. Wu, Scr. Mater. 55 (2006) 311.
[9] S.H. Chang, S.K. Wu, Mater. Trans. 48 (2007) 2143.
[10] P.J. Webster, K.R.A. Ziebeck, S.L. Town, M.S. Peak, Philos. Mag. 49 (1984) 295.
[11] V.V. Kokorin, V.A. Chernenko, Phys. Met. Metallogr. 68 (1989) 111.
[12] V.A. Chernenko, E. Cesari, V.V. Kokorin, I.N. Vitenko, Scr. Metall. Mater. 33 (1995) 1239.
[13] S.K. Wu, S.T. Yang, Mater. Lett. 57 (2003) 4291.
[14] V.A. Chernenko, J. Pons, C. Seguí, E. Cesari, Acta Mater. 50 (2002) 53.
[15] E. Cesari, V.A. Chernenko, V.V. Kokorin, J. Pons, C. Seguí, Acta Mater. 45 (1997) 999.
[16] C. Seguí, E. Cesari, J. Pons, V. Chernenko, Mater. Sci. Eng. A 370 (2004) 481.
[17] G. Fan, K. Otsuka, X. Ren, F. Yin, Acta Mater. 56 (2008) 632.
[18] S.H. Chang, S.K. Wu, Mater. Charact. 59 (2008) 987.
[19] A. Böhm, S. Roth, G. Naumann, W.G. Drossel, R. Neugebauer, Mater. Sci. Eng. A 481–482 (2008) 266.
[20] I. Aaltio, M. Lahelin, O. Söderberg, O. Heczko, B. Löfgren, Y. Ge, J. Seppälä, S.P. Hannula, Mater. Sci. Eng. A 481–482 (2008) 314.
[21] S.H. Chang, S.K. Wu, J. Alloys Compd. 459 (2008) 155.